translation $\tau < 10^{-4}$ s. This spectrum proves that the three possible long-axis orientations of *p*-xylene in the ZSM-5 channel system are occupied with near identical probability.

Appendix

We sketch here the derivation of the shift anisotropy pattern of Figure 2a, in which further narrowing of axially symmetric powder patterns is achieved by the jumping of molecules between selected orientations. We are concerned with the channel system of zeolite ZSM-5 (Figure 3), where smaller side channels are perpendicular to the straight main channels. This geometry can lead to unequal likelihood of occupation of the three orientations. Let the probability that the molecular unique axis lies parallel to the straight channel be p. Then the probability that this unique axis lies parallel to either one of the side-channel orientations is $(1 - p)/2$. Let the side channels make an acute angle α with each other. We compute the *averaged tensor* resulting from the translational diffusion process whereby a molecule, bearing such axially symmetric tensors for its nuclei, oriented in each channel as described above, makes random jumps from one channel, i.e., orientation, to another sufficiently rapidly so that motional averaging occurs. The geometry of the problem, i.e., Figure 3, suggests that the new principal axes will be as follows: axis 1 (principal value δ_{11}), in the plane of the undulating channels and bisecting the acute angle α; axis 2 (δ_{22}), also in that plane and perpendicular to axis 1; and axis 3 (δ_{33}), parallel to the axis of the straight channels. Rotations of the tensor were carried out by standard methods.[3,4,17]

Weighted averages along the expected principal axes are

$$\delta_{11} = \delta_\perp + (1 - p)(\delta_\parallel - \delta_\perp) \cos^2 (\alpha/2)$$

$$\delta_{22} = \delta_\perp + (1 - p)(\delta_\parallel - \delta_\perp) \sin^2 (\alpha/2)$$

$$\delta_{33} = \delta_\parallel - (1 - p)(\delta_\parallel - \delta_\perp)$$

$$\delta_{ij}(i \neq j) \equiv 0$$

Here $\delta_\parallel$ and $\delta_\perp$ are the principal values of the original axially symmetric tensor. The off-diagonal elements average to zero, confirming the choice of principal axes.

For equal probability of occupation of the three orientations, $p = {}^1/_3$, and

$$\delta_{11} = \bar{\delta} + (1/3)(\delta_d vt - \delta_\perp) \cos \alpha$$

$$\delta_{22} = \bar{\delta} - (1/3)(\delta_\parallel - \delta_\perp) \cos \alpha$$

$$\delta_{33} = \bar{\delta}$$

where $\bar{\delta} = (2\delta_\perp + \delta_\parallel)/3$, the average shift. Note that for $\alpha = \pi/2$, the expected isotropic shift results. These equations for the principal values were used to calculate the spectra of Figure 2a, applying them to the on-axis ring carbons, the off-axis ring carbons, and the methyl carbons. Variation of the occupation probability p in the range ${}^1/_4$–${}^1/_2$ moves the center peak only ±3 ppm. Similar formulas hold for NMR dipolar pair[18] interactions and to spin–1 quadrupolar interactions as well; in such cases a "mirror" spectrum of equal intensity, obtained by reflection of the spectrum about $\bar{\delta}$, must be added to the spectrum calculated from the above principal values.

Registry No. *o*-Xylene, 95-47-6; *p*-xylene, 106-42-3.

(17) J. F. Nye, "The Physical Properties of Crystals", Oxford University Press, London, 1957, p 24.

(18) N. K. Moroz, A. M. Panich, and S. P. Gabuda, *J. Struct. Chem. (Engl. Transl.)*, **19**, 293 (1976).

Relative Rate Constants for the Reactions of Atomic Oxygen with HO_2 and OH Radicals

Leon F. Keyser

Molecular Physics and Chemistry Section, Jet Propulsion Laboratory, California Institute of Technology, Pasadena, California 91109
(Received: August 18, 1982)

Relative rate constants for the reactions $O + HO_2 \rightarrow OH + O_2$ (1) and $O + OH \rightarrow H + O_2$ (2) were obtained by using the discharge-flow resonance fluorescence technique at 2 torr total pressure and 299 K. HO_2 radicals were generated by reacting atomic hydrogen with an excess of O_2. Quasi-steady-state concentrations of OH and HO_2 were established in the presence of excess atomic oxygen. Observed concentration ratios, $[OH]/[HO_2]$, resulted in a value of 1.7 ± 0.2 for k_1/k_2. The error limits are twice the standard deviation obtained from the data analysis. Overall experimental error is estimated to be ±25%. This result confirms earlier direct measurements of k_1 and k_2 which required knowledge of absolute radical or atomic oxygen concentrations.

Introduction

In the mesosphere and upper stratosphere, above about 35 km, HO_x radicals are rapidly interconverted by reactions with atomic oxygen (eq 1 and eq 2 followed by eq 3).[1-4] In

$$O + HO_2 \rightarrow OH + O_2 \quad (1)$$

$$O + OH \rightarrow H + O_2 \quad (2)$$

$$H + O_2 + M \rightarrow HO_2 + M \quad (3)$$

these regions of the atmosphere, the rate constant ratio, k_1/k_2, is an important factor in determining the relative concentrations of OH and HO_2.[1] Indeed above 50 km, $[OH]/[HO_2]$ is controlled almost entirely by the k_1/k_2 ratio.

Previous measurements of k_1/k_2 yielded values of (0.86 ± 0.4)[5] and 0.83.[6] These results are not consistent with

(1) Nicolet, M. *Rev. Geophys. Space Phys.* **1975**, *13*, 593.
(2) Allen, M.; Yung, Y. L.; Waters, J. W. *J. Geophys. Res.* **1981**, *86*, 3617.
(3) Prather, M. J. *J. Geophys. Res.* **1981**, *86*, 5325.
(4) Logan, J. A.; Prather, M. J.; Wofsy, S. C.; McElroy, M. B. *Phil. Trans. R. Soc., Ser. A* **1978**, *290*, 187.
(5) Hack, W.; Preuss, A. W.; Temps, F.; Wagner, H. Gg. *Ber. Bunsenges. Phys. Chem.* **1979**, *83*, 1275.

0022-3654/83/2087-0837$01.50/0

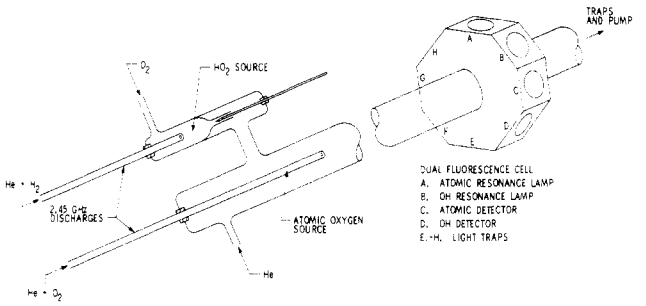

Figure 1. Schematic drawing of the discharge-flow resonance fluorescence apparatus. HO_2 was generated in a fixed reactor on the high-pressure side of a glass needle valve. Atomic oxygen was generated in a movable source by using a 2.45-GHz discharge of O_2 in helium. A dual fluorescence cell allowed simultaneous detection of atomic oxygen and OH. HO_2 was detected after quantitatively converting it to OH with excess NO.

recent absolute determinations of k_1 and k_2. Near 300 K the absolute studies yielded $(6.1 \pm 0.6) \times 10^{-11}$[7] and $(5.4 \pm 0.9) \times 10^{-11}$[8] cm^3 molecule^{-1} s^{-1} for k_1 and $(3.4 \pm 0.6) \times 10^{-11}$,[9] $(3.5 \pm 0.3) \times 10^{-11}$,[10] and $(3.2 \pm 0.5) \times 10^{-11}$[11] cm^3 molecule^{-1} s^{-1} for k_2. Using the average values of $(5.8 \pm 0.5) \times 10^{-11}$ cm^3 molecule^{-1} s^{-1} for k_1 and $(3.4 \pm 0.3) \times 10^{-11}$ cm^3 molecule^{-1} s^{-1} for k_2 yields (1.7 ± 0.2) for k_1/k_2. The difference between the ratio calculated from the absolute studies and the value obtained by the earlier relative measurements lies outside the combined experimental errors of both sets of measurements. This is so even if more realistic experimental errors of ±25% are assigned to each study. Possible reasons for the difference include (a) unrecognized secondary reactions or (b) errors in determining the absolute concentrations of atomic oxygen, OH, or HO_2.

In the present study k_1/k_2 was measured by using the discharge flow resonance fluorescence technique. Reactions 1–3 were used to form quasi-steady-state concentrations of OH and HO_2 in the presence of excess atomic oxygen. Concentration ratios of OH to HO_2 were used to determine k_1/k_2. In these experiments absolute concentrations of atomic oxygen, OH, or HO_2 were not needed. Thus, they serve as an independent verification of the absolute determinations of k_1 and k_2 which required a knowledge of actual HO_2,[7,8] atomic oxygen,[9,10] or OH[11] concentrations.

Experimental Section

The present study was carried out by using a fast-flow system with resonance fluorescence detection which is shown schematically in Figure 1. Details of this apparatus have been discussed earlier.[7,12] The 50.4-mm diameter flow tube was coated with a halocarbon wax to minimize wall losses of reactive species. A dual resonance fluorescence cell allowed simultaneous detection of OH radicals and atomic species.

HO_2 Source. HO_2 radicals were formed at a fixed point upstream of the main reaction zone. Atomic hydrogen produced in a microwave discharge of H_2 in helium was reacted with an excess of O_2 (eq 3). Under typical conditions in the source, $[O_2] = 2.2 \times 10^{17}$ cm^{-3} with [He] = 4.7×10^{17} cm^{-3} (total pressure = 21.3 torr at 298 K). A OH flow rate of approximately 45 cm^3 atm s^{-1} at 298 K was used. In the 15.6-mm diameter reactor this resulted in a flow velocity of about 840 cm s^{-1}. Complete reaction of atomic hydrogen was assured by allowing reaction 3 to proceed for about 6.5 ms before expansion into the main reaction zone which was operated at 2 torr total pressure. The ratio of concentrations in the HO_2 source to those in the main reactor was approximately 13 to 1. Initial concentrations of HO_2 in the main reaction zone were 3×10^{11}–4×10^{11} cm^{-3} with background OH typically less than 1×10^{10} cm^{-3} and atomic hydrogen less than 5×10^9 cm^{-3}.

Detector Calibrations. OH radicals were observed by using resonance fluorescence near 308 nm. HO_2 was detected after quantitatively converting it to OH by adding an excess of NO (eq 16). Although absolute concentrations

$$HO_2 + NO \rightarrow OH + NO_2 \qquad (16)$$

of OH, HO_2, atomic oxygen, and atomic hydrogen were not required for the present experiments, approximate concentrations were needed to assess the importance of secondary reactions and to make small corrections for radical losses during the HO_2 to OH conversion (see discussion below). The OH detector was calibrated by reacting a known concentration of NO_2 with an excess of atomic hydrogen (eq 17). Sensitivities were defined in terms of

$$H + NO_2 \rightarrow OH + NO \qquad (17)$$

OH concentrations at the NO addition port, $[OH]_p$. That is

$$S(OH)^- = I_c^-/[OH]_p \qquad (I)$$

$$S(OH)^+ = I_c^+/[OH]_p \qquad (II)$$

where I_c was the fluorescence intensity observed during the calibration runs. The superscripts refer to the absence or presence of NO. Because of slightly increased OH loss in the presence of NO, $S(OH)^+$ was less than $S(OH)^-$. By defining the sensitivities in this way, radical losses which are present both during the calibration and experimental runs tend to cancel. Details of this procedure have been given earlier.[7,12]

Atomic hydrogen was monitored by using resonance fluorescence at 121.6 nm. Signals were calibrated by converting the H atoms to OH with an excess of NO_2 (eq 17). Atomic oxygen was detected by using resonance fluorescence near 130.6 nm and calibrated by titrating with NO_2 (eq 18). Details of this procedure have been discussed by others.[9]

$$O + NO_2 \rightarrow NO + O_2 \qquad (18)$$

Reagents. Gases used were chromatographic grade helium (99.9999%), research grade hydrogen (99.9995%), ultrahigh-purity oxygen (99.95%), and nitric oxide (99.0%). The nitric oxide was purified by passage through a molecular sieve (Linde 13X) trap at 195 K. Nitrogen dioxide was prepared from nitric oxide by adding a large excess of oxygen. After several hours the oxygen was removed by slowly passing the mixture through a 195 K trap. The nitrogen dioxide was stored at 77 K and distilled to a 195 K trap before use. The chromatographic helium was passed through a molecular sieve (Linde 3A) trap at 77 K just prior to use.

Data Analysis

The present experiments were carried out at 299 K and 2 torr total pressure. In the main reaction zone, partial pressures of 0.5 torr of O_2 and 1.5 torr of helium were used.

(6) Burrows, J. P.; Cliff, D. I.; Harris, G. W.; Thrush, B. A.; Wilkinson, J. P. T. *Proc. R. Soc. London, Ser. A* **1979**, *368*, 463.
(7) Keyser, L. F. *J. Phys. Chem.* **1982**, *86*, 3439.
(8) Sridharan, U. C.; Qiu, L. X.; Kaufman, F. *J. Phys. Chem.* **1982**, *86*, 4569.
(9) Lewis, R. S.; Watson, R. T. *J. Phys. Chem.* **1980**, *84*, 3495.
(10) Howard, M. J.; Smith, I. W. M. *J. Chem. Soc., Faraday Trans. 2* **1981**, *77*, 997.
(11) Westenberg, A. A.; de Haas, N.; Roscoe, J. M. *J. Phys. Chem.* **1970**, *74*, 3431.
(12) Keyser, L. F. *J. Phys. Chem.* **1981**, *85*, 3667.

TABLE I: Reactions Occurring in the System Used to Determine k_1/k_2

no.	reaction	rate constant at 298[a]
1	$O + HO_2 \rightarrow OH + O_2$	6.1×10^{-11} [b]
2	$O + OH \rightarrow H + O_2$	3.3×10^{-11}
3a	$H + O_2 + O_2 \rightarrow HO_2 + O_2$	5.5×10^{-32} [c]
3b	$H + O_2 + He \rightarrow HO_2 + He$	1.6×10^{-32} [c]
4a	$H + HO_2 \rightarrow 2\ OH$	6.6×10^{-11} [d]
4b	$H + HO_2 \rightarrow H_2O + O$	3.1×10^{-12} [d]
4c	$H + HO_2 \rightarrow H_2 + O_2$	7.8×10^{-12} [d]
5	$OH + HO_2 \rightarrow H_2O + O_2$	6.4×10^{-11} [e]
6	$OH + OH \rightarrow H_2O + O$	1.9×10^{-12}
7	$HO_2 + HO_2 \rightarrow H_2O_2 + O_2$	1.0×10^{-12}
8	$OH + H_2O_2 \rightarrow HO_2 + H_2O$	1.7×10^{-12}
9	$OH + wall \rightarrow Products$	$11\ s^{-1}$ [f]
10	$HO_2 + wall \rightarrow Products$	$5\ s^{-1}$ [f]
11a	$O + O_2 + O_2 \rightarrow O_3 + O_2$	6.1×10^{-34} [c,g]
11b	$O + O_2 + He \rightarrow O_3 + He$	3.5×10^{-34} [c,g]
12	$O + O_3 \rightarrow 2\ O_2$	8.8×10^{-15}
13	$H + O_3 \rightarrow OH + O_2$	2.9×10^{-11}
14	$OH + O_3 \rightarrow HO_2 + O_2$	6.8×10^{-14}
15	$HO_2 + O_3 \rightarrow OH + 2\ O_2$	2.0×10^{-15}
16	$HO_2 + NO \rightarrow OH + NO_2$	8.3×10^{-12}
17	$H + NO_2 \rightarrow OH + NO$	1.3×10^{-10}
18	$O + NO_2 \rightarrow O_2 + NO$	9.3×10^{-12}
19	$H + NO + He \rightarrow HNO + He$	2.0×10^{-32} [c]
20	$OH + HNO \rightarrow H_2O + NO$	7.0×10^{-11}
21	$H + HNO \rightarrow H_2 + NO$	1.0×10^{-13}
22	$OH + NO + He \rightarrow HONO + He$	3.8×10^{-31} [c]
23	$OH + NO_2 + He \rightarrow HONO_2 + He$	9.2×10^{-31} [c]
24	$O + NO + He \rightarrow NO_2 + He$	6.2×10^{-32} [c]
25	$O_3 + NO \rightarrow O_2 + NO_2$	1.8×10^{-14}
26	$OH + H_2 \rightarrow H_2O + H$	7.5×10^{-15}

[a] Unless otherwise indicated, units are cm^3 molecule^{-1} s^{-1} and values were obtained from ref 13-15. [b] Reference 7. [c] cm^6 molecule^{-2} s^{-1}. [d] References 8 and 16. [e] Reference 12. [f] Measured. [g] Reference 17.

Atomic oxygen was in large excess over OH and HO_2. Under these conditions, the chemistry can be adequately described by reactions 1-15 given in Table I. Then

$$d[OH]/dt + [OH]\{k_2[O] + k_5[HO_2] + 2k_6[OH] + k_9\} = [HO_2]\{k_1[O] + 2k_{4a}[H]\} + k_{13}[H][O_3] \quad \text{(III)}$$

$$\frac{k_1}{k_2} = \frac{[OH]}{[HO_2]} \frac{\{1 + S\}}{\{1 + T\}} \quad \text{(IV)}$$

where

$$S = \frac{k_5[HO_2] + 2k_6[OH] + k_9}{k_2[O]}$$

$$T = \frac{2k_{4a}[H][HO_2] + k_{13}[H][O_3] - d[OH]/dt}{k_1[O][HO_2]}$$

Terms corresponding to reactions 8, 14, and 15 have been omitted from eq III and IV since they make negligible contributions to OH loss or production. Since atomic oxygen was in large excess, eq IV reduces to

$$k_1/k_2 \approx [OH]/[HO_2] \quad \text{(V)}$$

In each set of experiments, HO_2 was reacted with excess atomic oxygen until approximate steady-state concentrations of OH and HO_2 were established. The experimentally observed quantities were OH fluorescence intensities in the absence or presence of NO. The intensity observed without added NO, I^-, was proportional to [OH]

$$I^- = [OH]S(OH)^- \quad \text{(VI)}$$

while the fluorescence intensity with added NO, I^+, was proportional to [OH] + $[HO_2]$

$$I^+ = \{[OH] + [HO_2]\}S(OH)^+ \quad \text{(VII)}$$

Then

$$\frac{[OH]}{[HO_2]} = \left\{\frac{I^+}{I^-}\frac{S(OH)^-}{S(OH)^+} - 1\right\}^{-1} \quad \text{(VIII)}$$

Equation VIII demonstrates that absolute OH detector calibrations were not required for the present measurements. The sensitivity ratio, $S(OH)^-/S(OH)^+$, was determined by turning the NO flow off and on at a fixed [OH]. Results ranged from 1.06 to 1.10. An average value of 1.08 was used to calculate $[OH]/[HO_2]$.

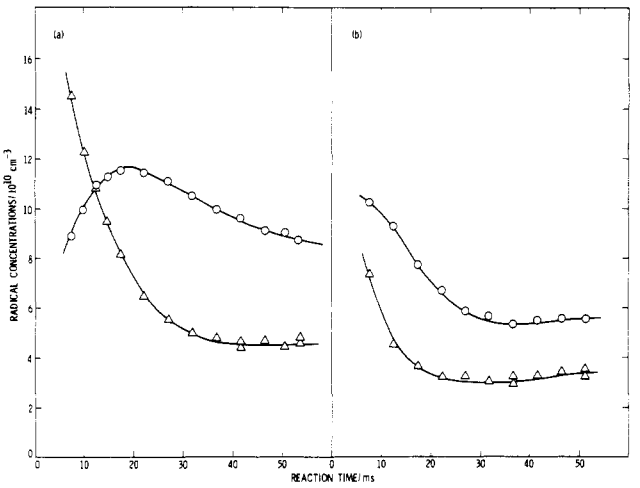

Figure 2. Radical concentrations vs. reaction time: O, [OH]; Δ, $[HO_2]$; (a) [O] = 1.7×10^{12} cm^{-3}, (b) [O] = 4.2×10^{12} cm^{-3}. Estimated errors in the concentrations are ±25%.

Results and Discussion

Time profiles of OH and HO_2 are shown in Figure 2. Although they are not needed to determine $[OH]/[HO_2]$, absolute concentrations are given in the plots. Experimental conditions and results are summarized in Table II. The $[OH]/[HO_2]$ ratios shown in column 4 were obtained from fluorescence intensity ratios in the steady-state region by using eq VIII. At the low atomic oxygen concentration used in experiment 1, the OH maximum occurred at an experimentally accessible reaction time. For this experiment $[OH]/[HO_2]$ is also given at maximum [OH].

Corrections for OH loss (or production) which was present during the experimental runs but was not present during the calibrations were applied to the observed fluorescence intensities used in eq VIII. These corrections (less than 8%) were obtained from computer simulations of the experimental and calibration runs by using the reactions and rate constants given in Table I. Details of this procedure were discussed earlier.[7]

Atomic hydrogen was present at steady-state concentrations between 1×10^{11} and 3×10^{11} cm^3 during the ratio experiments. When excess NO was added to convert HO_2 to OH by reaction 16, NO_2 was produced. The NO_2 converted some of the atomic hydrogen to OH by reaction 17. This additional OH produced from NO_2 was included in the computer simulations used to calculate corrections for OH loss or production between the NO port and the OH

(13) DeMore, W. B.; Golden, D. M.; Hampson, R. F.; Howard, C. J.; Kurylo, M.; Molina, M. J.; Ravishankara, A. R.; Watson, R. T. Jet Propulsion Laboratory, California Institute of Technology, Pasadena, CA, 1982, JPL Publication 82-57.
(14) Baulch, D. L.; Cox, R. A.; Hampson, R. F., Jr.; Kerr, J. A.; Troe, J.; Watson, R. T. *J. Phys. Chem. Ref. Data* **1980**, *9*, 295.
(15) Hampson, R. F. Washington, DC; 1980, Federal Aviation Administration Report No. FAA-EE-80-17.
(16) Keyser, L. F., results to be published.
(17) Lin, C. L.; Leu, M. T. *Int. J. Chem. Kinet.* **1982**, *14*, 417, and references cited therein.

TABLE II: Summary of Results

$\bar{\nu}$, cm s^{-1}	$10^{-12} \times$ [O], cm^{-3}	reaction time, ms	$[OH]/[HO_2]^{a,b}$	$k_1/k_2{}^{c,b}$
		Experiment 1[d]		
1028	1.73	53	1.88	
		53	1.92	
		50	2.07	
		46	1.98	
		42	2.11	
		42	2.21	
		av	2.0 ± 0.2	1.9 ± 0.2
at maximum [OH],		19 ± 2	1.5	1.6
		Experiment 2[d]		
981	2.76	54	1.94	
		54	1.92	
		49	1.84	
		44	1.85	
		39	2.05	
		39	1.92	
		34	2.05	
		av	1.9 ± 0.2	1.8 ± 0.2
		Experiment 3[d]		
1000	3.72	48	1.96	
		43	1.85	
		38	1.86	
		33	2.00	
		33	1.80	
		28	1.98	
		av	1.9 ± 0.2	1.7 ± 0.2
		Experiment 4[d]		
1025	4.20	51	1.71	
		51	1.69	
		46	1.71	
		42	1.75	
		37	1.75	
		37	1.91	
		32	1.93	
		27	1.92	
		av	1.8 ± 0.2	1.7 ± 0.2
		Experiment 5[d]		
980	5.85	49	1.75	
		49	1.98	
		44	1.72	
		38	1.96	
		38	1.79	
		33	2.01	
		28	1.76	
		23	1.89	
		av	1.9 ± 0.2	1.7 ± 0.2
			overall av	1.7 ± 0.2

[a] From eq VIII with $S(OH)^-/S(OH)^+ = 1.08$. Observed fluorescence intensities were corrected for OH loss or production (see text) using the following factors for I^- and I^+, respectively: expt 1, 1.00, 1.01; expt 2, 0.98, 1.04; expt 3, 0.98, 1.06; expt 4, 0.98, 1.06; expt 5, 0.97, 1.08. [b] Errors are twice the standard deviation. [c] From $[OH]/[HO_2]$ after correcting for secondary reactions by using eq IV. [d] In the steady-state region, the average concentrations of atomic hydrogen, OH, HO_2, and O_3 were, respectively, as follows: expt 1, 1.49×10^{11}, 9.15×10^{10}, 4.61×10^{10}, 3.44×10^{10} cm^{-3}; expt 2, 1.99×10^{11}, 6.60×10^{10}, 3.57×10^{10}, 5.42×10^{10} cm^{-3}; expt 3, 2.89×10^{11}, 6.17×10^{10}, 3.33×10^{10}, 7.76×10^{10} cm^{-3}; expt 4, 2.54×10^{11}, 5.56×10^{10}, 3.28×10^{10}, 7.62×10^{10} cm^{-3}; expt 5, 2.65×10^{11}, 3.95×10^{10}, 2.34×10^{10}, 1.01×10^{11} cm^{-3}. Atomic hydrogen and OH concentrations were observed by using resonance fluorescence and HO_2 by conversion to OH with NO. Ozone concentrations were obtained from computer simulations.

detector (see above). However, NO_2 impurities in the NO could also produce additional OH and lead to an overestimate of $[HO_2]$ and, thus, an underestimate of k_1/k_2. To test for NO_2 impurities, excess NO was added to atomic hydrogen while monitoring the OH fluorescence intensity. For these experiments $[H] = 2.4 \times 10^{11}$ cm^{-3} and $[NO] = 2.4 \times 10^{14}$ cm^{-3}. The NO was added 3-ms upstream of the OH detector to duplicate conditions used during the k_1/k_2 measurements. The [OH] generated upon addition of NO was found to be $(2 \pm 1) \times 10^9$ cm^{-3}. For a 3-ms reaction time between the NO port and OH detector, this corresponds to initial $[NO_2] = (2.0 \pm 1.0) \times 10^{10}$ cm^{-3} or an impurity level of 1×10^{-4}. Estimates of [OH] generated from NO_2 impurities in NO were made by using $[NO_2] = 2 \times 10^{10}$ cm^{-3}, $k_{17} = 1.3 \times 10^{-10}$ cm^3 $molecule^{-1}$ s^{-1}, and steady-state atomic hydrogen concentrations observed during the ratio experiments. The resulting [OH] given in units of molecules cm^{-3} are as follows: expt 1, 1.1×10^9; expt 2, 1.5×10^9; expt 3, 2.1×10^9; expt 4, 1.9×10^9; expt 5, 2.0×10^9. The $[OH]/[HO_2]$ ratios given in Table II have been corrected for this additional OH production from NO_2. These corrections were less than 10%.

The rate constant ratio, k_1/k_2, given in column 5 of Table II was obtained from the $[OH]/[HO_2]$ ratios by using eq IV. This corrects for contributions from secondary reactions and nonsteady-state OH. For these calculations atomic hydrogen, OH, HO_2, and O_3 concentrations given in note *d* of Table II were used. The effect of nonsteady-state OH was negligible except at the relatively low atomic oxygen concentrations used in experiments 1 and 2 where it was included.

The resulting average value for k_1/k_2 is 1.7 ± 0.2 where the errors are twice the standard deviation. Overall experimental error is estimated to be ±25%. The present result is in excellent agreement with the rate constant ratio, k_1/k_2, calculated by using the previously determined values of the individual rate coefficients.[7-11] This confirms these earlier absolute determinations and demonstrates that the difficult measurements of absolute HO_2, OH, and atomic oxygen concentrations required in these studies were substantially correct. Previous measurements of the k_1/k_2 ratio do not agree with the present study and the absolute determinations of k_1 and k_2. Possible reasons for this difference are discussed below.

Burrows et al.[6] measured k_1/k_2 and k_1/k_8 by observing maximum OH and HO_2 generated from the reaction of atomic oxygen with H_2O_2 (eq 27). The values obtained

$$O + H_2O_2 \rightarrow OH + HO_2 \qquad (27)$$

for these ratios were 0.83 and 37, respectively. However, their results become internally inconsistent when recently measured values of k_8[18-20] are used to calculate k_1. This suggests that the reaction mechanism used in the data analysis was not complete. For example, wall loss of OH and the reaction of HO_2 with atomic hydrogen were not included. Since the observed wall loss of OH was very high (30–70 s^{-1}), its omission could have a significant effect on their results. Moreover, concentrations of atomic oxygen required in their analysis were determined in separate experiments and not at the maximum [OH] and $[HO_2]$. Since OH and HO_2 were continuously generated and their concentrations were approximately 1×10^{11} cm^{-3} or greater in these experiments, significant loss of atomic oxygen could have occurred between the point at which it was determined and the time at which [OH] and $[HO_2]$ reached their maximum values.

Hack et al.[5] used a discharge-flow system with laser magnetic resonance and electron spin resonance detection

(18) Keyser, L. F. *J. Phys. Chem.* **1980**, *84*, 1659.
(19) Sridharan, U. C.; Reimann, B.; Kaufman, F. *J. Chem. Phys.* **1980**, *73*, 1286.
(20) Wine, P. H.; Semmes, D. H.; Ravishankara, A. R. *J. Chem. Phys.* **1981**, *75*, 4390.

to determine k_1/k_2. The method used to generate HO_2 and OH was the same as that used in the present study. However, Hack et al. used larger concentrations of atomic oxygen (2×10^{13} cm^{-3} < [O] < 3×10^{14} cm^{-3}) and chose to measure k_1/k_2 by observing [OH]/[HO_2] only at the point where [OH] reached its maximum. They did not observe ratios in the quasi-steady-state region. Their result was $k_1/k_2 = 0.86 \pm 0.4$. Computer simulations of these experiments using conditions given in their Table 3 show that maximum [OH] occurred at 1 ms or less and that at this time [HO_2] was falling rapidly. Thus, it was very difficult to accurately determine [OH]/[HO_2] in this way. In addition, an estimate of the mixing time in their system using the relation $t = R^2/2D$, with $R = 1.5$ cm and $D = 170$ cm^2 s^{-1} (diffusion coefficient of atomic oxygen in helium at 4.5 torr)[21] results in 6-7 ms. This suggests that mixing may not have been complete at the time the [OH] maximum was observed.

(21) Marrero, T. R.; Mason, E. A. *J. Phys. Chem. Ref. Data* **1972**, *1*, 3.

Conclusions

The rate constant ratio, k_1/k_2, was found to be 1.7 ± 0.4 which is in excellent agreement with the ratio calculated by using earlier independent determinations of k_1 and k_2. This confirms the absolute rate constant measurements which required experimentally difficult determinations of absolute radical or atomic oxygen concentrations. These results are expected to have a significant effect on predicted concentrations of atomic oxygen, O_3, and HO_x in the mesosphere and upper stratosphere above 35 km.[7,8]

Acknowledgment. The research described in this paper was performed at the Jet Propulsion Laboratory, California Institute of Technology, under contract with the National Aeronautics and Space Administration.

Registry No. Atomic oxygen, 17778-80-2; hydroxyl, 3352-57-6; hydroperoxo, 3170-83-0.

Muonium Addition to Cyanides

J. M. Stadlbauer,* B. W. Ng, Y. C. Jean,† and D. C. Walker

Department of Chemistry and TRIUMF, University of British Columbia, Vancouver, British Columbia V6T 1Y6, Canada

(Received: September 14, 1982)

Muonium, the light radioactive isotope of hydrogen, was found to add to the C≡N bond of acetonitrile, cyanoacetate, cyanide, and tetracyanocadmate(II) with room temperature rate constants, k_M, of 5.1×10^7, 7.7×10^7, 3.0×10^9, and 1.7×10^{10} (all M^{-1} s^{-1}), respectively. While $Cd(CN)_4^{2-}$ is diffusion controlled with a critical energy of ~15 kJ/mol, the others appear to be activation controlled as with cyanoacetate's activation barrier of ~35 kJ/mol. Kinetic isotope effects range from 0.7 to 24.

Introduction

Muonium (Mu) is an atom-like particle consisting of a positive muon nucleus (μ^+) with a bound electron. Though the mass of Mu is 1/9 that of H the reduced masses are nearly equal giving Mu an ionization potential and Bohr radius similar to H. Because the muon nucleus is a radioactive particle with an intrinsic lifetime of 2.2×10^{-6} s, muonium can be used as a probe to directly observe hydrogen-atom reactions. Due to the factor of 9 difference between the masses of Mu and H, Mu should be an excellent particle to study kinetic isotope effects.

Muonium is formed when an energetic muon (4.1-28 MeV) enters the target and abstracts an electron from the stopping medium into a bound state. The muon itself is a product of a positive pion (π^+) decay which in turn is a product of a proton capture by ^{9}Be. When the muon decays it ejects a positron which can be easily observed and counted by using nuclear physics counting techniques. More detailed descriptions of the particles and techniques are available elsewhere.[1,2]

Muonium was originally observed to form in gases.[3] Later, pure liquids such as water,[4] alcohols,[5,6] and certain hydrocarbons[7,8] were found to produce usable amounts of muonium with long enough lifetimes (up to 20 μs in water[9]) to be useful as solvents to study a diverse number of solutes more reactive toward muonium. In water such reactions as addition, abstraction, oxidation-reduction, and spin conversion can be observed and measured.[2] When analogous hydrogen atom reactions have been measured the kinetic isotope effect can be calculated.

In a previous study we observed the addition reactions of Mu with several vinyl monomers[10] reporting isotope effects of 1.1 and 2.8 for acrylamide and acrylonitrile, respectively. In an effort to obtain a better understanding of muonium addition reaction isotope effects we selected cyanide, both organic and inorganic forms, as the reactive solute. ESR studies[11,12] have established that both organic and inorganic cyanides undergo addition by H; therefore Mu should also add across the C≡N bond of cyanide.

†Department of Physics, University of Missouri—Kansas City, Kansas City, MO 64110

(1) D. G. Fleming, D. M. Garner, L. C. Vaz, D. C. Walker, J. H. Brewer, and K. M. Crowe, *Adv. Chem. Ser.*, **No. 175**, 279 (1979).
(2) D. C. Walker, *J. Phys. Chem.*, **85**, 3960 (1981).
(3) V. W. Hughes, *Annu. Rev. Nucl. Sci.*, **16**, 445 (1966).
(4) P. W. Percival, H. Fischer, M. Camani, F. N. Gygax, W. Ruegg, A. Schenck, H. Schilling, and H. Graf, *Chem. Phys. Lett.*, **39**, 333 (1976).
(5) P. W. Percival, E. Roduner, and H. Fischer, *Adv. Chem. Ser.*, **No. 175**, 335 (1979).
(6) P. W. Percival, E. Roduner, H. Fischer, M. Camani, F. N. Gygax, and A. Schenck, *Chem. Phys. Lett.*, **47**, 11 (1977).
(7) Y. Ito, B. W. Ng, Y. C. Jean, and D. C. Walker, *Can. J. Chem.*, **58**, 2395 (1980).
(8) B. W. Ng, J. M. Stadlbauer, Y. C. Jean, and D. C. Walker, *Can. J. Chem.*, in press.
(9) K. Nagamine, K. Nishiyama, J. Imazato, H. Nakayuama, M. Yoshida, Y. Sakai, H. Sato, and T. Tominaga, *Chem. Phys. Lett.*, **87**, 186 (1982).
(10) J. M. Stadlbauer, B. W. Ng, D. C. Walker, Y. C. Jean, and Y. Ito, *Can. J. Chem.*, **59**, 3261 (1981).
(11) P. Neta and R. W. Fessenden, *J. Phys. Chem.*, **74**, 3362 (1970).
(12) D. Behar and R. W. Fessenden, *J. Phys. Chem.*, **76**, 3945 (1972).

0022-3654/83/2087-0841$01.50/0